Molecular simulation of adsorption of *n*-alkanes in Na-MFI zeolites. Determination of empirical expressions.

E. García-Pérez[a], I. M. Torréns[a], S. Lago[a], R. Krishna[b], B. Smit,[b] and S. Calero[a].

[a] Department of Environmental Sciences, University Pablo de Olavide, Ctra Utrera km1. 41013 Seville, Spain.

[b] Department of Chemical Engineering, University of Amsterdam, Nieuwe Achtergracht 166, 1018 WV Amsterdam, The Netherlands.

We performed Configurational-Bias Monte Carlo simulations to provide adsorption isotherms, Henry coefficients and heats of adsorption of alkanes in sodium exchanged MFI- and MOR-type zeolites. We derived empirical expressions from the simulation data to describe the adsorption of linear alkanes in sodium exchanged MFI structures. These expressions adequately describe the Henry coefficient and adsorption enthalpy of *n*-alkanes as a function of sodium density and temperature. In the high coverage regime we provide an expression for saturation capacities of *n*-alkanes in the zeolite that combined with the obtained for Henry coefficients, gives a direct estimation of the complete adsorption isotherms of pure adsorbents and mixtures.

1. INTRODUCTION

Molecular simulations using classical potential models provide molecular level information inaccessible to experiment and beyond the reach of ab initio calculations. In particular, Configurational-Bias Monte Carlo (CBMC) simulations are capable of accurately predicting adsorption of alkanes in zeolites [1-6] and Molecular dynamics simulations using similar potentials can also predict diffusivities that closely match experiment [7]. MFI and MOR-type topologies are among the most important synthetic zeolites from an industrial point of view [8-10]. MOR exists in a large Si/Al ratio domain and therefore it is particularly useful for catalytic applications. The structure with the highest Al-content has a composition $Na_8Al_8Si_{40}O_{96}$ and the structure can be refined with *Cmcm* symmetry [11]. The framework has a porous structure, which consists of main channels parallel to [001], having a slightly elliptical cross section with 12 TO_4 tetrahedron units (T = Si, Al), which are connected with small side channels parallel to [010], with 8 TO_4 cross sections called side-pockets.

The MFI-type zeolite can be synthesized with a composition range $8 \leq Si/Al \leq \infty$. It is a three-dimensional pore system consisting of straight, 0.53 nm across parallel channels intersected by perpendicular zigzag channels and with 10-membered rings of oxygen atoms controlling the entrance to the channels [9]. At room temperature this zeolite typically has an orthorhombic symmetry (space group *Pnma*) with 12 distinct crystallographic T-sites [12]. In a previous work we presented a new force field able to reproduce accurately adsorption properties in sodium exchanged faujasites zeolites [13,14]. In this work we demonstrate that

this force field can be successfully extended to other sodium exchanged zeolites. Firstly we have performed molecular simulations to provide adsorption properties of *n*-alkanes in several Na-MOR and Na-MFI structures varying the non-framework sodium concentration and secondly we have fitted the obtained results for Na-MFI structures with an empirical expression for Henry coefficients and heats of adsorption as a function of the sodium concentration, temperature, and type of alkane. Finally we have extended our calculations to mixtures of alkanes.

2. METHODS

Simulations in the low and high coverage regime were computed using Configurational- Bias Monte Carlo (CBMC) in the grand-canonical and NVT ensemble, respectively. The conventional simulation techniques to compute adsorption isotherms are prohibitively expensive for long alkanes whereas the CBMC technique simulates them at affordable cost [15]. In a CBMC simulation molecules are grown bead by bead biasing the growth process towards energetically favorable configurations avoiding overlap with the zeolite. During the growth the Rosenbluth factor is calculated. The average Rosenbluth factor is directly related to the free energy and the Henry coefficients [14,16]. More details on this simulation technique can be found elsewhere [16-18].

Zeolite frameworks have been constructed from silicon, aluminium, and oxygen atoms. The MFI-type zeolites were modeled from the crystallographic structure of silicalite [10] in which Si atoms were substituted by Al atoms [19-20]. The MOR models have been constructed from the crystallographic data of Meier [11]. In all cases simulation boxes were chosen large enough to obey the minimum image convention with a potential cut-off of 12 Å and periodic boundary conditions were applied in all directions. The charge distribution on the oxygen framework was considered static; i.e. polarization of oxygen by nearby sodium cations is implicitly modeled by distinguishing silicon from aluminium with a difference of 0.3 e$^-$ between q_{Si} and q_{Al} [21]. Different charges are used for oxygen atoms bridging two silicon atoms, q_{OSi}, and oxygen atoms bridging one silicon and one aluminium atom q_{OAl}. q_{OSi} is obtained using the relation $q_{Si} + (2 \times q_{OSi}) = 0$, making the zeolite neutral in the absence of aluminium, while q_{OAl} is chosen to make the total system charge equal to zero [13, 22, 23].

The non-framework sodium cation density was adjusted to match the framework aluminium density and the density of the zeolites is determined by the framework atoms (aluminium, silicon and oxygen) and the non-framework cations (sodium). In our model, the sodium cations can move freely (interactions defined through Lennard-Jones and coulombic potentials) and adjust their position depending on their interactions with the framework atoms, other sodium cations, and alkane molecules.

The interactions between guest molecules (alkanes and sodium cations) with the zeolite host framework are modeled by Lennard-Jones and Coulombic potentials. The Coulomb interactions in the system are calculated using the Ewald summation [16]. The alkanes are described with a united atom model, in which CH_x groups are considered as a single interaction centers with their own effective potentials [24]. The beads in the chain are connected by harmonic bonding potentials. The bond bending between three neighbouring beads is modeled by a harmonic cosine bending potential and changes in the torsional angle are controlled by a Ryckaert-Bellemans potential. The beads in a chain separated by more than three bonds interact with each other through a Lennard-Jones potential. The interactions of the adsorbed molecules with the zeolite are dominated by the dispersive forces between the pseudo-atoms and the oxygen atoms of the zeolite [25-27] meaning that the silicon van der

Waals interactions are taken into account through an effective potential with only the oxygen atoms. We use a newly developed force field, where the nature, density, and mobility of the non-framework cation, the density of the framework aluminium, and all host-guest interactions are carefully taking into account. The alkane-sodium, alkane-alkane, and alkane-zeolite interaction parameters were obtained by calibrating the force field through explicitly fitting a full isotherm over a wide range of pressures, temperatures and sodium densities [13]. We fit complete adsorption isotherms, because experimental determination of the adsorption properties at very low and at very high coverage is fraught with difficulty resulting in a large spread in experimentally determined Henry coefficients and saturation loadings, respectively. The agreement between experimental data from different groups in the intermediate coverage regime is significantly better [13].

3. RESULTS AND DISCUSSION

Fig. 1a shows the excellent agreement of our computed isotherms for ethane in Na-MFI with available experimental data [28]. The isotherms reproduce the experimental isotherm shape and also the experimental saturation capacity of the validation data set. They were obtained for MFI structures with 3 Na$^+$/uc at 295 and 297 K, respectively. Henry coefficients and heats of adsorption of linear alkanes were computed for a wide range of temperatures and the full range of aluminium (and sodium) densities in both MOR and MFI-type zeolites. Table 1 summarizes the obtained values as a function of the sodium density for the MFI structure at 300K.
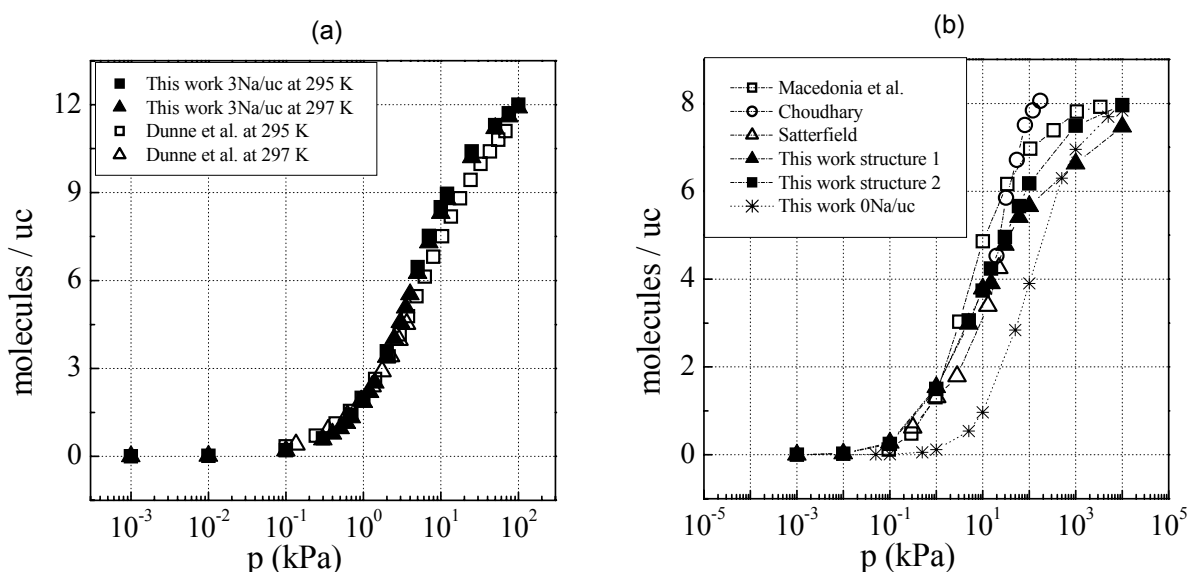

Fig. 1. Simulated adsorption isotherms of ethane in sodium-exchanged zeolites. Available previous data are included for comparison [4, 28-30]; (a) Na-MFI structures with 3 Na$^+$/uc at 295 and 297 K. (b) Na-MOR structures with 8Na$^+$/uc at 296 K.

Fig. 1b shows adsorption isotherms of ethane in sodium exchanged MOR structures (8Na$^+$/uc) at 296K. Differences between previous experimental data are clearly observed [4, 29,30]. Agreement between Maginn et al. [4] and Satterfield et al. [29] is good at low pressures but

their isotherms diverge above 10kPa. Choudhary et al. show higher adsorption for their range of pressures leading to presume that small differences in sample preparation and aluminium distribution can play an important role on the adsorption in MOR topologies. Our simulations support this theory showing variation on the adsorption isotherms of ethane in Na-MOR structures with different Al distribution. Fig. 1b additionally compares the adsorption of ethane in both, pure silica and Na-exchanged structures. At 10 kPa the ethane loading is about one molecule per unit cell for the former, increasing up to four molecules per unit cell for the later. Our previous results showed similar behaviour for Na-exchanged faujasites [6] and differences for MFI structures, though less significant, were also observed. This leads us to claim that non-framework sodium cations are vital to accurately obtain adsorption of alkanes in Na-exchanged zeolites.

As shown in Fig. 2, Henry coefficients of linear alkanes in sodium exchanged MFI topologies adequately fit on a surface defined through the expression:

$$LnK_H = (\eta \cdot Ns + v) \cdot CN - \xi \tag{1}$$

where η, v, and ξ are given in Table 2 for a wide range of temperatures. This temperature dependence is captured by:

$$z(T) = \frac{\left(\dfrac{x_1}{T} + x_2\right)}{T} + x_3 T, \quad z = \eta, v, \xi \tag{2}$$
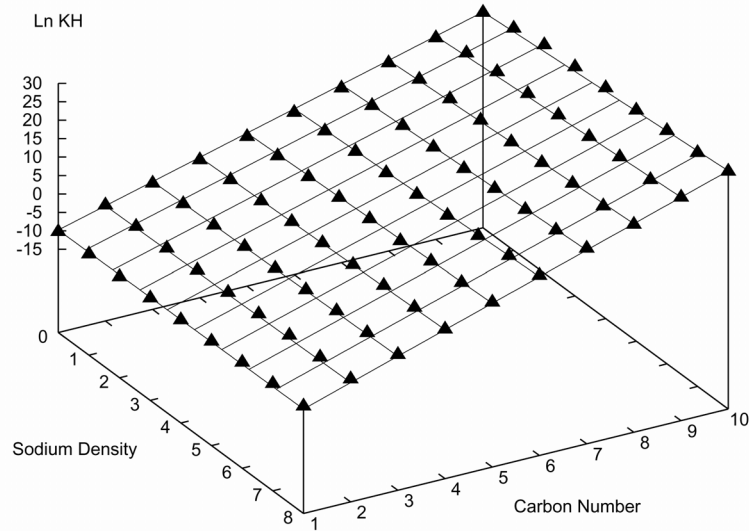
Fig. 2. Henry coefficients of *n*-alkanes in Na-MFI obtained using CBMC simulations. Henry coefficients were computed at 300 K and they are plotted as a function of carbon number (methane to decane) and as a function of sodium density.

Table 1.
Henry coefficients [molKg^{-1}Pa^{-1}] at 300K, and heats of adsorption [kJ/mol] in Na-MFI.

	2 Na/u.c.		4 Na/u.c.		6 Na/u.c		8 Na/u.c.	
	LnK$_H$	-ΔH°	LnK$_H$	-ΔH°	LnK$_H$	-ΔH°	LnK$_H$	-ΔH°
Methane	-11.8	18.6	-11.3	20.7	-10.7	22.6	-10.1	23.9
Ethane	-8.3	32.0	-8.0	32.9	-7.5	35.0	-7.2	36.1
Propane	-6.0	41.7	-5.5	43.2	-5.0	46.2	-4.6	47.2
Butane	-3.4	52.4	-2.8	55.0	-2.2	58.1	-1.8	59.3
Pentane	-0.8	62.4	-0.2	64.9	0.3	68.3	0.9	71.9
Hexane	2.0	73.4	2.5	74.9	3.1	79.6	4.0	84.4
Heptane	4.9	84.9	5.4	86.3	6.3	91.4	6.8	97.1
Octane	8.0	97.4	8.6	98.5	9.0	103.5	9.2	106.6
Nonane	11.1	110.0	11.7	110.7	12.1	116.0	12.0	119.2
Decane	14.4	122.2	15.0	122.9	15.1	128.2	15.1	131.9

Eqs. 1 and 2 can be combined into an empirical expression that describes the *n*-alkane Henry coefficient K_H [mol kg^{-1} Pa^{-1}] as a function of sodium density Ns [cations per unit cell], temperature T [K], and carbon number CN:

$$LnK_H = \frac{1}{2}[4387.72(Ns+10570)CN - 11487.2] + \frac{1}{2}[(5Ns+1166.4)CN + 1221.89] - $$
$$(0.016Ns+1.409)CN - 17.9 \tag{3}$$

The temperature derivative of Eq. 3 provides an expression for the adsorption enthalpy ΔH_0 [kJ/mol]:

$$\Delta H_0 = \frac{2}{}[(4387.72Ns+10570)CN - 11487.2] + (5Ns+1166.4)CN + 1221.89 \tag{4}$$

Table 2.
Coefficients η, ν, and ξ as a function of temperature.

T [K]	250	300	350	400	450	500
η	0.074	0.048	0.035	0.024	0.017	0.011
ν	342.42	26008	200.81	157.08	123.35	0.97
ξ	130.2	139.6	145.25	149.24	152.52	155.19

Fig. 3 compares the heats of adsorption of *n*-alkanes obtained from the empirical expression with available experimental data [31-35]. The applicability of the new force field is by no means limited to low pressure for it also reproduces accurately the adsorption of alkanes at high pressures [13]. The saturation capacities (θ_{sat}) of *n*-alkanes (methane to hexadecane) for

Na-exchanged MFI topologies can be fit to a second order exponential decay as a function of the carbon number (CN):

$$\theta_{sat}[molecules/uc] = 1.1 + 21.5exp-\left[\frac{CN}{2.7}\right] + 6.9exp-\left[\frac{CN}{13}\right] \tag{5}$$

$$\theta_{sat}[molecules/uc] = \theta_{sat}[mol \cdot kg^{-1}] \cdot N_{AV} \cdot [kg \cdot m^{-3}] \cdot [m^3] \tag{6}$$

Where N_{AV} is Avogadro's number, ρ the zeolite density and V is the volume of the unit cell.
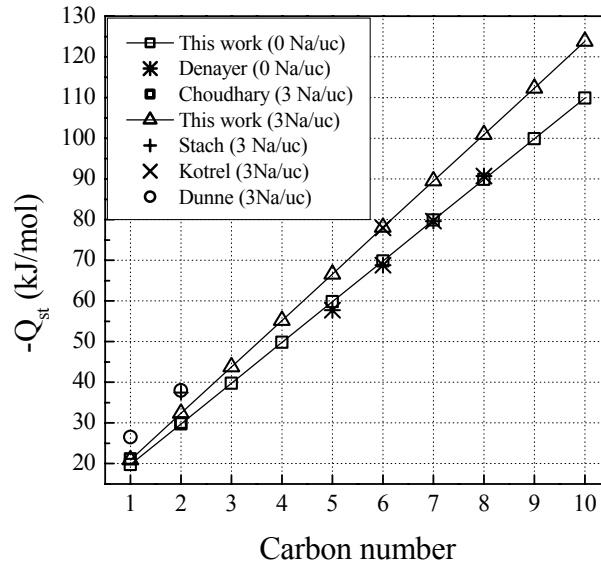

Fig. 3. Heats of adsorption of linear alkanes in Na-MFI zeolites obtained from our empirical expression. In all cases deviation between empirical (Eq. 4) and computed results is smaller than the symbol size. Available experimental sets are included for comparison [31-35].

The saturation capacity [mol kg^{-1}] combined with the expression for the Henry coefficients (Eq. 3) allow the direct estimation of the adsorption isotherms of linear alkanes in sodium MFI structures by using the Langmuir isotherm in the form:

$$\theta = \frac{K_H kp}{1 + (K_H / \theta_{sat})p} \tag{7}$$

Where θ is the loading of alkane in the zeolite in mol per kilogram and p is the system pressure in Pa. Calculations using Eq. 7 are in good agreement with the adsorption isotherms of adsorbents obtained from CBMC in silicalite and sodium exchanged structures. This can be observed in Fig. 4 for the adsorption of pure component methane, ethane, propane and n-butane and the equimolar quaternary mixture in MFI at 300 K.
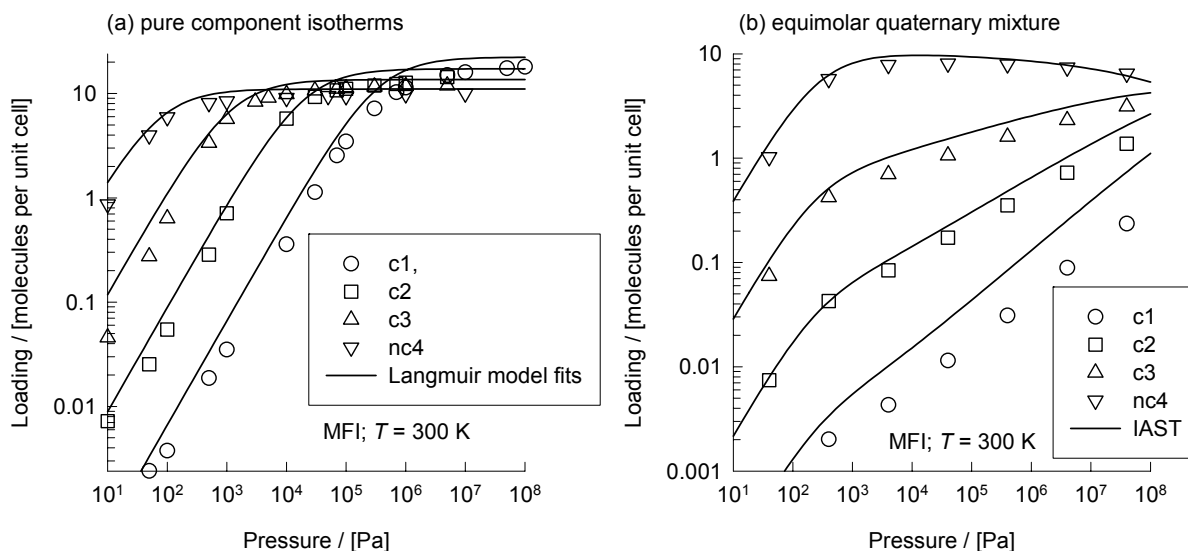
Fig. 4. Adsorption isotherms of n-alkanes in MFI using 1) CBMC simulation (symbols) and 2) a Langmuir model in which the parameters are calculated from Eqs. 3 and 5 (line). Left: Pure components. Right: Equimolar mixture of methane, ethane, propane and n-butane.

4. CONCLUSIONS

Our recently developed united atom force field for alkanes in sodium faujasites has been successfully applied to a variety of MOR and MFI sodium exchanged topologies. In the low coverage regime we provide simple expressions that adequately describe the n-alkane Henry coefficient and adsorption enthalpy in Na-MFI topologies as a function of sodium density and temperature. The predicted Henry coefficients and heats of adsorption compare extremely well to available experimental data affording an adequate substitute for complex Configurational-Bias Monte Carlo simulations. In the high coverage regime we provide an expression for saturation capacities of linear alkanes in sodium exchanged MFI. This expression combined with the expression for the Henry coefficients gives a direct estimation of adsorption isotherms of pure adsorbents and mixtures, in good agreement with the adsorption isotherms obtained from CBMC.

AKNOWLEDGEMENTS

REFERENCES

[1] V. Lachet, A. Boutin, B. Tavitian, and A. H. Fuchs, Faraday Discuss., (1997) 307.
[2] R. Krishna, B. Smit, and T. J. H. Vlugt, J. Phys. Chem. A., 102 (1998) 7727.
[3] C. F. Mellot, A. K. Cheetham, S. Harms, S. Savitz, R. J. Gorte, and A. L. Myers, J. Am. Chem. Soc., 120 (1998) 5788.

[4] M. D. Macedonia, D. D. Moore, and E. J. Maginn, Langmuir, 16 (2000) 3823.

[5] S. Calero, B. Smit, and R. Krishna, Phys. Chem. Chem. Phys., 3 (2001) 4390.

[6] R. Krishna, B. Smit, and S. Calero, Chem. Soc. Rev., 31 (2002) 185.

[7] S. M. Auerbach, J. Kärger, and S. Vasenkov. Diffusion in Zeolites, Marcel Dekker Inc., New York, 2003. pp.341-422.

[8] D. H. Olson, G. T. Kokotailo, S. L. Lawton, and W. M. Meier, J. Phys. Chem., 85 (1981) 2238.

[9] E. M. Flanigen, J. M. Bennet, J. M. Grose, R. W. Cohen, J. P. Patton, R. L. Kirchen, and R. M. Smith, Nature, 271 (1978) 512.

[10] H. van Koningsveld, H. van Bekkum, and J. C. Jansen, Acta Crystallogr., Sect. B, 43 (1987) 127.

[11] W. M. Meier, Kristallografiya, 115 (1961) 439.

[12] C. Baerlocher, W. M. Meier, and D. H. Olson. Atlas of zeolite framework types. Elsevier, London, 2001.

[13] S. Calero, D. Dubbeldam, R. Krishna, B. Smit, T. J. H. Vlugt, J. F. M. Denayer, J. A. Martens, and T. L. M. Maesen, J. Am. Chem. Soc., 126 (2004) 11377.

[14] D. Dubbeldam, S. Calero, T. L. M. Maesen, and B. Smit, Phys. Rev.Lett., 90 (2003) No.245901

[15] B. Smit and T. Maesen, Nature, 374 (1995) 42.

[16] D. Frenkel and B. Smit. Understanding Molecular Simulation. Academic Press, San Diego, CA, 2002.

[17] R. J. H. Vlugt, R. Krishna, and B. Smit, J. Phys. Chem. B, 103 (1999) 1102.

[18] B. Smit and J. I. Siepmann, J. Phys. Chem., 98 (1994) 8442.

[19] M. S. Stave and J. B. Nicholas, J. Phys. Chem., 99 (1995) 15046.

[20] A. E. Alvarado-Swaisgood, M. K. Barr, P. J. Hay, and A. Redondo, J. Phys. Chem., 95 (1991) 10031.

[21] E. Jaramillo and S. M. Auerbach, J. Phys. Chem. B, 103 (1999) 9589.

[22] E. Beerdsen, B. Smit, and S. Calero, J. Phys. Chem. B, 106 (2002) 10659.

[23] E. Beerdsen, D. Dubbeldam, B. Smit, T. J. H. Vlugt, and S. Calero, J. Phys. Chem. B, 107 (2003) 12088.

[24] J. P. Ryckaert and A. Bellemans, Faraday Discuss. Chem. Soc., 66 (1978) 95.

[25] A. G. Bezus, A. V. Kiselev, A. A. Lopatkin, and Q. D. Pham, J. Chem. Soc., Faraday Trans. 2, 74 (1978) 367.

[26] A. V. Kiselev, A. A. Lopatkin, and A. A. Shulga, Zeolites, 5 (1985) 261.

[27] T. J. H. Vlugt, R. Krishna, and B. Smit, J. Phys. Chem. B, 103 (1999) 1102.

[28] J. A. Dunne, M. Rao, S. Sircar, R. J. Gorte, and A. L. Myers, Langmuir, 12 (1996) 5896.

[29] C. N. Satterfield and A. J. Frabetti, AIChE J., 13 (1967) 731.

[30] A. L. Choudhari, S. Mayadevi, and A. Pai Singh, J. Chem. Soc., Faraday Trans., 91 (1995) 2935.

[31] J. A. Dunne, M. Rao, S. Sircar, R. J. Gorte, and A. L. Myers, Langmuir, 13 (1997) 4333.

[32] H. Stach, K. Fiedler, and J. Janchen, Pure Appl. Chem., 65 (1993) 2193.

[33] S. Kotrel, M. P. Rosynek, and J. H. Lunsford, J. Phys. Chem. B, 103 (1999) 818.

[34] J. F. Denayer, W. Souverijns, P. A. Jacobs, J. A. Martens, and G. V. Baron, J. Phys. Chem. B, 102 (1998) 4588.

[35] V. R. Choudhary and S. Mayadevi, Sep. Sci. Technol., 28 (1993) 2197.

[36] J. F. M. Denayer and G. V. Baron, Adsorption-J. Int. Adsorpt. Soc., 3 (1997) 251.